Response to Referee #1 (Dr. Kleinen)

We would like to thank Dr. Kleinen for his thoughtful and constructive review. Our responses to all of the referee's comments (italicized) are presented below.

In their manuscript, the authors present a model study of soil carbon accumulation in Alaska over the last 15000 years with a special focus on peat carbon accumulation. Compared to the authors' original submission I find the manuscript improved. However, a few issues remain. This review of the revised version was, by the way, hindered by the fact that the "track changes" version of the manuscript changes was different from the submitted revision, therefore not showing the actual changes to the manuscript. I would also suggest to the authors to use the "compare documents" function the next time, since that shows differences between versions more clearly. In my first review, one of my points was "Page 4, lines 94-95: the Spahni et al. Model has actually been evaluated with respect to the variables listed – see Wania et al. Publications on the LPJ-Why model on which Spahni is based." The authors have changed the passage I indicated to "In contrast, Spahni et al. (2013) used a dynamic global vegetation and land surface process model (LPX), based on LPJ (Sitch et al., 2003), imbedded with a peatland module, which considered the nitrogen feedback on plant productivity (Xu-Ri and Prentice, 2008) and plant biogeography, to simulate the SOC accumulation rates of northern peatlands. However, the model did not consider methane dynamics, which play an important role in affecting peat carbon dynamics, presumably due to its inadequate representation of ecosystem processes (Stocker et al., 2011, 2014; Kleinen et al., 2012). Furthermore, climatic effects on SOC were not fully explained." Obviously the authors did not actually read the literature. The LPX model does indeed consider methane dynamics (Spahni et al., Biogeosciences, 2011 and Zürcher et al., Biogeosciences, 2013). In addition this statement is wrong in another way, since methane dynamics actually are not important at all in the peat carbon uptake, which is what the authors focus on in their manuscript. This passage needs revisiting. (Page 4, line 91 to page 5, line 97).

We deleted those statements and only left the statement of "Climatic effects on SOC were not fully explained, presumably due to its inadequate representation of ecosystem processes".

Furthermore, I asked the authors to provide a table with site locations used in their assessment at site level – instead they added a reference, which is inadequate. The aim of my request was to enable readers to quickly understand where these sites are, without requiring the original publications. In addition, the discussion of site results is lacking some of the detail contained in the original manuscript.

In this revision, we added a table (Table 5) of the description of the four sites we used for site-level comparison. To make the manuscript more concise and focused, we decided not to discuss much on the site-level comparison in the Result and Discussion Section, since those results have

already been presented and discussed in our previous study (Wang et al, 2016). Therefore, we only showed the modeled results along with a brief discussion for those four sites in this study.

I also asked the authors to describe how the change in peatland extent was determined. However, I was unfortunately not able to understand that from the description in the paper (page 9, lines 188-205). I understand the link between basal age and peatland extent the authors used to determine changes in peatland area, but that is very difficult to understand from the text since the connection is not made clearly. Please reformulate to make it clearer.

We have added few more sentences and reformulated to make such method clearer to readers.

Page 13, line 277 refers to table 4, but this is table 2 in the revised version. I have not been able to check whether all other references to changed Figures and Tables are correct – I suggest the authors check this again before final publication.

Thanks for pointing this out. Correct, here we should have referred to Table 2 instead of Table 4. In this revision, we checked all the references to figures and tables.

Response to Referee #2 (Dr. Tupek)

We would like to thank Dr. Tupek for his thoughtful and constructive review, as well as his detailed comments. Our responses to all of the referee's comments are provided as below.

General comments:

Authors accounted for the required changes satisfactorily and the manuscript has improved. It is not clear if the long-term variation in NPP is larger than the inter-annual NPP variation (Fig. 5). Please explain the reasons for the large NPP inter-annual variation. Is it annual variation in climate? One of the main findings is that vegetation distributions drives soil C. To me it seems that climate is driving vegetation distribution which determines soil C change. However, long-term vegetation distribution here is taken from maps produced for main periods of climatic change thus introducing large step wise changes. This is also interesting result. Consider reformulating.

Yes, the inter-annual NPP variation depends on the annual variation of climate. As key factors controlling plant productivity are monthly temperature, solar radiation, and precipitation, their inter-annual fluctuations affect NPP. However, despite the large inter-annual NPP variation, we can still see a clear trend of long-term increasing (or decreasing) NPP from 15 ka to 19th. The 1000-year average NPP of those several vegetation types mostly reached the highest during the HTM period. To make it clear for readers, we added a third panel in Fig. 5 to represent this long-term feature. The result of carbon dynamics indeed shows large step-wise changes due to vegetation distribution shift. We directly applied the vegetation maps, which were generated in previous study, and were discussed regarding the generating process of those maps along with the uncertainty analyses (He et al., 2014).

Specific comments:

lines 32-34, reformulate, especially the origin of previous estimates is not obvious

We added "using peat core data" to give a brief idea how the previous estimates have been done and the references and origin of the previous estimates were then discussed in Section 3.3.

lines 41-44 in abstract and lines 463-467 in conclusions are identical, reformulate or delete

In this revision, we revised the sentences in the Conclusion Section to avoid duplication.

lines 374-378 explain reasons for long-term variation and inter annual variation of NPP (Fig. 5).

We added the explanation of the reason causing inter-annual NPP variation here and made clearer that it was the trend of long-term NPP coincided with the warmer climate, higher vegetation C and soil C stocks during the HTM.

Fig. 4 use same x axis; add a,b,c,d to the panels; Kenai Gasfield mismatch?

We added those letters to each panel. We also used the same scale for x axis in each panel. We confirmed that there was no mismatch for Kenai Gasfield. The highest 500-years average rate

occurred during 11-10.5 ka, as shown in the bar. We added "14.5-5 ka" in the caption to make the bar clearer to read.

Fig. 5 what is the reason for the large NPP inter-annual variation? add smoothed dashed line for higlighting the longterm changes?

We added the reason in the text and added a separate panel (Figure 5c) to show the long-term changes of NPP.

Fig.6 use same color codes as Fig. 5

We applied the same color code to Fig. 6.

Fig.7 use same color codes as Fig. 8?

We used the same color code in Fig. 7.

Fig. 9 "the area of…0 km2" confusing/delete, divide SP and SBP peatlands?

We deleted this confusing sentence.

Fig. 10 Peat C stock change. Specify that these are barplots to avoid confusion that peat C stock change is restricted to zero?

We specified that the plots are bars.

Quantifying Soil Carbon Accumulation in Alaskan Terrestrial Ecosystems during the Last 15,000 Years

Sirui Wang[1], Qianlai Zhuang[1,2*], Zicheng Yu[3]

[1]Department of Earth, Atmospheric, and Planetary Sciences, Purdue University, West Lafayette, Indiana, 47907

[2]Department of Agronomy, Purdue University, West Lafayette, IN 47907

[3]Department of Earth and Environmental Sciences, Lehigh University, Bethlehem, PA 18015

Correspondence to: qzhuang@purdue.edu

Abstract: Northern high latitudes contain large amounts of soil organic carbon (SOC), in which Alaskan terrestrial ecosystems account for a substantial proportion. In this study, the SOC accumulation in Alaskan terrestrial ecosystems over the last 15,000 years was simulated using a process-based biogeochemistry model for both peatland and non-peatland ecosystems. Comparable with the previous estimates of 25-70 Pg C in peatland and 13-22 Pg C in non-peatland soils within 1-m depth in Alaska using peat core data, our model estimated a total SOC of 36-63 Pg C at present, including 27-48 Pg C in peatland soils and 9-15 Pg C in non-peatland soils. Current vegetation stored 2.5-3.7 Pg C in Alaska with 0.3-0.6 Pg C in peatlands and 2.2-3.1 Pg C in non-peatlands. The simulated average rate of peat C accumulation was 2.3 Tg C yr^{-1} with a peak value of 5.1 Tg C yr^{-1} during the Holocene Thermal Maximum (HTM) in the early Holocene, four folds higher than the average rate of 1.4 Tg C yr^{-1} over the rest of the Holocene. The SOC accumulation slowed down, or even ceased, during the neoglacial climate cooling after the mid-Holocene, but increased again in the 20th century. The model-estimated peat depths ranged from 1.1 to 2.7 m, similar to the field-based estimate of 2.29 m for the region. We found that the changes in vegetation and their distributions were the main factors to determine the spatial variations of SOC accumulation during different time periods. Warmer summer temperature and stronger radiation seasonality, along with higher precipitation in the HTM and the 20th century might have resulted in the extensive peatland expansion and carbon accumulation.

Keywords: Carbon, Peatlands, Alaska, Modelling, Climate

1. Introduction

Global surface air temperature has been increasing since the middle of the 19th century (Jones and Mogberg, 2003; Manabe and Wetherald, 1980, 1986). Since 1970, the warming trend has accelerated at a rate of 0.35 ℃ per decade in northern high latitudes (Euskirchen et al., 2007; McGuire et al., 2009). It is predicted that the warming will continue in the next 100 years (Arctic Climate Impact Assessment 2005; Intergovernmental Panel on Climate Change (IPCC), 2013, 2014). The land surface in northern high latitudes (>45° N) occupies 22% of the global surface and stores over 40% of the global soil organic carbon (SOC) (McGuire et al., 1995; Melillo et al., 1995; McGuire and Hobbie, 1997). Specifically, the northern high latitudes were estimated to store 200-600 Pg C (1 Pg C = 10^{15} g C) in peatland soils depending on the depth considered (Gorham, 1990, 1991; Yu, 2012), 750 Pg C in non-peatland soils (within 3 m) (Schuur et al., 2008; Tarnocai et al., 2009; Hugelius et al., 2014), and additional 400 Pg C in frozen loess deposits of Siberia (Zimov et al., 2006a). Peatland area is around 40 million hectares in Alaska compared with total 350 million hectares in northern high latitudes (Kivinen and Pakarinen, 1981). Alaskan peatlands account for the most peatland area in the USA and cover at least 8% of the total land area (Bridgham et al., 2006). To date, the regional soil C and its responses to the climate change are still with large uncertainties (McGuire et al., 2009; Loisel et al., 2014).

The warming climate could increase C input to soils as litters through stimulating plant net primary productivity (NPP) (Loisel et al., 2012). However, it can also decrease the SOC by increasing soil respiration (Yu et al., 2009). Warming can also draw down the water table in peatlands by increasing evapotranspiration, resulting in higher decomposition as the aerobic

198 respiration has a higher rate than anaerobic respiration in general (Hobbie et al., 2000). SOC
199 accumulates where the rate of soil C input is higher than decomposition. The variation of climate
200 may switch the role of soils between a C sink and a C source (Davidson and Janssens, 2006;
201 Davidson et al., 2000; Jobbagy and Jackson, 2000). Unfortunately, due to the data gaps of field-
202 measurement and uncertainties in estimating regional C stock (Yu, 2012), with limited
203 understanding of both peatlands and non-peatlands and their responses to climate change, there is
204 no consensus on the sink and source activities of these ecosystems (Frolking et al., 2011; Belyea,
205 2009; McGuire et al., 2009).

206 Both observation and model simulation studies have been applied to understand the long-
207 term peat C accumulation in northern high latitudes. Most field estimations are based on series of
208 peat-core samples (Turunen et al., 2002; Roulet et al., 2007; Yu et al., 2009; Tarnocai et al.,
209 2009). However, those core analyses may not be adequate for estimating the regional C
210 accumulation due to their limited spatial coverage. To date, a number of model simulations have
211 also been carried out. For instance, Frolking et al. (2010) developed a peatland model
212 considering the effects of plant community, hydrological dynamics and peat properties on SOC
213 accumulation. The simulated results were compared with peat-core data. They further analyzed
214 the contributions of different plant functional types (PFTs) to the peat C accumulation. However,
215 this 1-D model has not been evaluated with respect to soil moisture, water-table depth, methane
216 fluxes, and carbon and nitrogen fluxes and has not been used in large spatial-scale simulations by
217 considering other environmental factors (e.g., temperature, vapor pressure, and radiation). In
218 contrast, Spahni et al. (2013) used a dynamic global vegetation and land surface process model
219 (LPX), based on LPJ (Sitch et al., 2003), imbedded with a peatland module, which considered
220 the nitrogen feedback on plant productivity (Xu-Ri and Prentice, 2008) and plant biogeography,

to simulate the SOC accumulation rates of northern peatlands. ~~However, the model did not consider methane dynamics, which play an important role in affecting peat carbon dynamics, presumably due to its inadequate representation of ecosystem processes (Stocker et al., 2011, 2014; Kleinen et al., 2012). Furthermore,~~ However, c~~C~~climatic effects on SOC were not fully explained, presumably due to its inadequate representation of ecosystem processes (Stocker et al., 2011, 2014; Kleinen et al., 2012). The Terrestrial Ecosystem Model (TEM) has been applied to study C and nitrogen dynamics in the Arctic (Zhuang et al., 2001, 2002, 2003, 2015; He et al., 2014). However, the model has not been calibrated and evaluated with peat-core C data, and has not been applied to investigate the regional peatland C dynamics. Building upon these efforts, recently we fully evaluated the peatland version of TEM (P-TEM) including modules of hydrology (HM), soil thermal (STM), C and nitrogen dynamics (CNDM) for both upland and peatland ecosystems (Wang et al., 2016).

Here we used the peatland-core data for various peatland ecosystems to parameterize and test P-TEM (Figure 1). The model was then used to quantify soil C accumulation of both peatland and non-peatland ecosystems across the Alaskan landscape since the last deglaciation. This study is among the first to examine the peatlands and non-peatlands C dynamics and their distributions and peat depths using core data at regional scales.

2. Methods

2.1. Overview

To conduct regional simulations of carbon accumulation for both uplands and peatlands, we first parameterized the P-TEM for representative ecosystems in Alaska. Second, we

organized the regional vegetation and peatland distribution data, spatial basal age data for all peatland grid cells based on site-level soil core data, and climate data for each period during the Holocene. Finally, we conducted the regional simulations and sensitivity analysis.

2.2 Model Description

In P-TEM (Wang et al., 2016), peatland soil organic C (SOC) accumulation is determined by the difference between NPP and aerobic and anaerobic decompostion. Peatlands accumulate C where NPP is greater than decomposition, resulting in positive net ecosystem production (NEP):

$$NEP = NPP - R_H - R_{CH_4} - R_{CWM} - R_{CM} - R_{COM} \quad (1)$$

P-TEM was developed based on the Terrestrial Ecosystem Model (TEM) at a monthly step (Zhuang et al., 2003; 2015). It explicitly considers the process of aerobic decomposition (R_H) related to the variability of water-table depth; net methane emission after methane oxidation (R_{CH_4}); CO_2 emission due to methane oxidation (R_{CWM}) (Zhuang et al., 2015); CO_2 release accompanied with the methanogenesis (R_{CM}) (Tang et al., 2010; Conrad, 1999); and CO_2 release from other anaerobic processes (R_{COM}, e.g., fermentation, terminal electron acceptor (TEA) reduction) (Keller and Bridgham, 2007; Keller and Takagi, 2013). For upland soils, we only considered the heterotrohic respiration under aerobic condition (Raich, 1991). For detailed model description see Wang et al. (2016).

We modeled peatland soils as a two-layer system for hydrological module (HM) while keeping the three-layer system for upland soils (Zhuang et al., 2002). The soil layers above the lowest water table position are divided into: (1) moss (or litter) organic layer (0-10 cm); and (2)

humic organic layer (10-30 cm) (Wang et al., 2016). Based on the total amount of water content within those two unsaturated layers, the actual water table depth (WTD) is estimated. The water content at each 1 cm above the water table can be then determined after solving the water balance equations (Zhuang et al., 2004).

In the STM module, the soil vertical profile is divided into four layers: (1) snowpack in winter, (2) moss (or litter) organic layer, (3) upper and (4) lower humic organic soil (Wang et al., 2016). Each of these soil layers is characterized with a distinct soil thermal conductivity and heat capacity. We used the observed water content to drive the STM (Zhuang et al., 2001).

The methane dynamics module (MDM) (Zhuang et al., 2004) considers the processes of methanogenesis, methanotrophy, and the transportation pathways including: (1) diffusion through the soil profile; (2) plant-aided transportation; and (3) ebullition. The soil temperatures calculated from STM, after interpolation into 1-cm sub-layers, are input to the MDM. The water-table depth and soil water content in the unsaturated zone for methane production and emission are obtained from HM, and NPP is calculated from the CNDM. Soil-water pH is prescribed from observed data and the root distribution determines the redox potential (Zhuang et al., 2004).

2.3 Model Parameterization

We have parameterized the key parameters of the individual modules including HM, STM, and MDM in Wang et al. (2016). The parameters in CNDM for upland soils and vegetation have been optimized in the previous studies (Zhuang et al 2002, 2003; Tang and Zhuang 2008). Here we parameterized P-TEM for peatland ecosystems using data from a moderate rich *Sphagnum* spp. open fen (APEXCON) and a *Sphagnum*-black spruce (*Picea*

mariana) bog (APEXPER) (Table 1). Both are located in the Alaskan Peatland Experiment (APEX) study area, where *Picea mariana* is the only tree species above breast height in APEXPER. Three water table position manipulations were established in APEX including a control, a lowered, and a raised water table plots (Chivers et al., 2009; Turetsky et al., 2008; Kane et al., 2010; Churchill et al., 2011). There were also several internal collapse scars that formed with thaw of surface permafrost, including a non-, an old, and a new collapse plots. APEXCON represents the control manipulation and APEXPER represents the non-collapse plot. The annual NPP and aboveground biomass at both sites have been measured in 2009. There were no belowground observations at APEX, however at a Canadian peatland, Mer Bleue, which includes *Sphagnum* spp. dominated bog (dominated by shrubs and *Sphagnum*) and pool fen (dominated by sedges and herbs and *Sphagnum*). The belowground biomass was also observed at Suurisuo mire complex, southern Finland, a sedge fen site dominated by *Carex rostrate*. We used the ratio (70%) of belowground biomass to total biomass from these two study sites to calculate the missing belowground biomass values at APEXCON and APEXPER (Table 2). We conducted 100,000 Monte Carlo ensemble simulations to calibrate the model for each site using a Bayesian approach and parameter values with the modes in their posterior distributions were selected (Tang and Zhuang, 2008, 2009).

2.4 Regional Model Input Data

The Alaskan C stock was simulated through the Holocene driven with vegetation data reconstructed for four time periods including a time period encompassing a millennial-scale warming event during the last deglaciation known as the BØlling-AllerØd at 15-11 ka (1 ka =

1000 cal yr Before Present), HTM during the early Holocene at 11-10 and 10-9 ka, and the mid- (9-5 ka) and late- Holocene (5 ka-1900 AD) (He et al., 2014). We used the modern vegetation distribution for the simulation during the period 1900-2000 AD (Figure 2). We assumed that the vegetation distribution remained static within each corresponding time period. Upland ecosystems were classified into boreal deciduous broadleaf forest, boreal evergreen needleleaf and mixed forest, alpine tundra, wet tundra; and barren lands (Table 3). By using the same vegetation distribution map, we reclassified the upland ecosystems into two peatland types including *Sphagnum* spp. poor fens (SP) dominated by tundra and *Sphagnum* spp.-black spruce (*Picea mariana*) bog/ peatland (SBP) dominated by forest ecosystems (Table 3).

Upland and peatland ecosystem distribution for each grid cell was determined using the wetland inundation data extracted from the NASA/ GISS global natural wetland dataset (Matthews and Fung, 1987). The resolution was resampled to 0.5°×0.5° from 1°×1°. Given the same topography of Alaska during the Holocene, we assumed that the wetland distribution kept the same throughout the Holocene. The inundation fraction was assumed to be the same within each grid through time and the land grids not covered by peatland were treated as uplands. We calculated the total area of modern Alaskan peatlands to be 302,410 km^2, which was within the range from 132,000 km^2 (Bridgham et al., 2006) to 596,000 km^2 (Kivinen and Pakarinen, 1981). The soil water pH data were extracted from Carter and Scholes (2000), and the elevation data were derived from Zhuang et al. (2007).

Our regional simulations considered the effects of basal ages on carbon accumulation. To obtain the spatially explicit basal age data for all peatlands grid cells, we first categorized the observed basal ages of peat samples from Gorham et al. (2012) into different time periods including ~~corresponding to the periods in this study (e.g.,~~ 15-11 ka, 11-10 ka, 10-9 ka, and 9 ka-

19th). (Figure 2). For During each time period, we then categorized the areas dominated with different vegetation types were assigned with varying spatial distribution of peatland basal ages into the areas was correlated with the dominated by different vegetation types. To do that, we examined the association of peat basal ages and vegetation types from peat core data. We assumed that the peatland started initiation in ing on the certain vegetation areas where the largest number of peat basal age points fall within. For instance, we found that peatland initiations during 15-11 ka occurred in the regionspixels that were dominated by alpine tundra at south, northwestern, and southeastern coast. We thus assign linkedused the vegetation types withto estimate the different peatland basal ages for the grid cells according to their with corresponding vegetation types for for all grid cells at regional scales during each time slice (Table 4).

Formatted: Superscript

Climate data were bias-corrected from ECBilt-CLIO model output (Timm and Timmermann, 2007) to minimize the difference from CRU data (He et al., 2014). Climate fields include monthly precipitation, monthly air temperature, monthly net incoming solar radiation, and monthly vapor pressure at resolution of 2.5°×2.5°. We used the same time-dependent forcing atmospheric carbon dioxide concentration data for model input as were used in ECBilt-CLIO transient simulations from the Taylor Dome (Timm and Timmermann, 2007). The historical climate data used for the simulation through the 20th century were monthly CRU2.0 data (Mitchell et al., 2004).

2.5 Simulations and Sensitivity Test

Simulations for pixels located on the Kenai Peninsula from 15 to 5 ka were first conducted with the parameterized model. The peat-core data from four peatlands on the Kenai Peninsula, Alaska (Jones and Yu, 2010; Yu et al., 2010) (Table 5, also see Table 3 in Wang et al. (2016) ~~Table 3~~) were used to compare with the simulations. The observed data include the peat depth, bulk density of both organic and inorganic matters at 1-cm interval, and age determinations. The simulated C accumulation rates represent the actual ("true") rates at different times in the past. However, the calculated accumulation rates from peat cores are considered as "apparent" accumulation rates, as peat would continue to decompose since the time of formation until present when the measurement was made (Yu, 2012). To facilitate comparison between simulated and observed accumulation rates, we converted the simulated "true" accumulation rates to "apparent" rates, following the approach by Spahni et al. (2013). That is, we summed the annual net C accumulation over each 500-year interval and deducted the total amount of C decomposition from that time period, then dividing by 500 years.

Second, we conducted a transient regional simulation driven with monthly climatic data (Figure 3) from 15 ka to 2000 AD. The simulation was conducted assuming all grid cells were taken up by upland ecosystems to get the upland soil C spatial distributions during different time periods. We then conducted the second simulation assuming all grid cells were dominated by peatland ecosystems following Table 3 to obtain the distributions of peat SOC accumulation. Finally, we used the inundation fraction map to extract both uplands and peatlands and estimated the corresponding SOC stocks within each grid, which were then summed up to represent the Alaskan SOC stock. We also used the observed mean C content of 46.8% in peat mass and bulk density of 166 ± 76 kg m^{-3} in Alaska (Loisel et al., 2014) to estimate peat depth distribution from the simulated peat SOC density (kg C m^{-2}).

Third, we conducted a series of extra simulations to further examine how uncertain climates and vegetation distribution affect our results. We used the original forcing data as the standard scenario and the warmer (monthly temperature $+5℃$) and cooler ($-5℃$) as other two scenarios while keeping the rest forcing data unchanged. Similarly, we used the original forcing data as the standard scenario and the wetter (monthly precipitation $+10$ mm) and drier (-10 mm) to test the effect from precipitation. To further study if vegetation distribution has stronger effects on SOC accumulation than climate in Alaska, we simply replaced SBP with SP and replaced the upland forests with tundra at the beginning of 15 ka. We then conducted the simulation under "warmer" and "wetter" conditions simultaneously as described before while keeping the vegetation distribution unchanged.

3. Results and Discussion

3.1 Simulated Peatland Carbon Accumulation Rates at Site Level

Our paleo simulations showed a large peak of peat C accumulation rates at 11-9 ka during the HTM (Figure 4). The simulated "true" and "apparent" rates captured this primary feature in peat-core data at almost all sites (Jones and Yu, 2010; See Wang e al. (2016) Table 3 for sites details). We simulated an average of peat SOC "apparent" accumulation rate of 11.4 g C m^{-2} yr^{-1} from 15 to 5 ka, which was slightly higher than the observations at four sites (10.45 g C m^{-2} yr^{-1}). The simulated rate during the HTM was 26.5 g C m^{-2} yr^{-1}, up to five times higher than the rest of the Holocene (5.04 g C m^{-2} yr^{-1}). This corresponded to the observed average rate of 20 C m^{-2} yr^{-1} from 11.5 to 8.6 ka, which is, four times higher than 5 C m^{-2} yr^{-1} over the rest of the Holocene.

3.2 Vegetation Carbon

Model simulations showed an overall low vegetation C before the HTM (15-11 ka) (Figure 5a), paralleled to the relatively low annual and long-term NPP (Figures 5b and c). The lowest amount of C (~0.8 kg C m^{-2}) was stored in *Sphagnum*-dominated peatland. *Sphagnum*-black spruce peatland also had low vegetation C density (~1 kg C m^{-2}). Upland vegetation showed a generally higher C storage, among which boreal evergreen needleleaf forest ranked the first (~2 kg C m^{-2}). Highest NPP accompanied by highest vegetation carbon appeared during the HTM (11-9 ka) (Figures 5a and b). Lower annual C uptake along with lower C was found during mid- and late- Holocene (9 ka-19th), where peatland ecosystems exhibited the most obvious drops (Figures 5a and b).

In general, vegetation held about 2 Pg C before the HTM (Figure 6). Upland tundra ecosystems accounted for the most amount of C. During the HTM, Boreal evergreen needleleaf forest reached its highest and had an overwhelming proportion over total C. Similarly, a peak of total vegetation C appeared at the same time, averaging around 4.3 Pg C. Large decrease occurred at the mid-Holocene and a slight decline continued till the late-Holocene. We estimated a total 2.9 Pg C stored in modern Alaskan vegetation, with 0.4 Pg in peatlands and 2.5 Pg in non-peatlands. The uncertainties during the model calibration (Table 2~~4~~) resulted in 0.3-0.6 Pg C and 2.2-3.1 Pg C in peatlands (see Wang et al. (2016) for model parameters) and non-peatland vegetation (see Tang and Zhuang (2008) for uncertainty analyses for upland vegetation), respectively. Our estimation of 2.5-3.7 Pg C stored in the Alaskan vegetation was lower than the previous estimate of 5 Pg (Balshi et al., 2007; McGuire et al., 2009), presumably due to the prior ranges of model parameters used from Tang and Zhuang (2008). Our overestimation of peatland area may also lead to a reduction of Alaskan non-peatland area.

420

421 **3.3 Soil Carbon**

422 Carbon storage in Alaskan non-peatland soils varied spatially (Figure 7). Moist tundra
423 had the highest SOC density (12-25 kg C m^{-2}), followed by deciduous broadleaf forest (8-13
424 kg C m^{-2}) and evergreen needleleaf forest (3-8 kg C m^{-2}) through all time slices between 15 ka
425 and 2000 AD. Dramatic changes of vegetation types have occurred in Alaska during different
426 periods (Figure 2). Before the HTM (15-11 ka), the terrestrial ecosystem was dominated by
427 tundra. Northwestern coast and eastern interior was covered by moist tundra. Southwestern
428 Alaska and the interior south of the Brooks Range were dominated by alpine tundra (Figure 2a).
429 The basal ages of peat samples from Gorham et al. (2012) suggested that peatlands were likely to
430 form from the (alpine) tundra ecosystems, although patches of boreal deciduous broadleaf forest
431 and boreal evergreen needleleaf and mixed forest appeared at the north of the Alaska Range.
432 Initially, only *Sphagnum* open peatland (SP) existed, with less C (<10 kg C m^{-2}) sequestrated in
433 the southeastern Brooks Range in comparison with southwestern and northwestern coastal parts
434 (>15 kg C m^{-2}) (Figure 8a). Approximately 4.5×10^5 km^2 area was covered by peatlands at the
435 beginning of the HTM (~11 ka) (Figure 9). During the HTM (11-9 ka), boreal deciduous
436 broadleaf and boreal evergreen needleleaf and mixed forests expanded (Figures 8b and c).
437 Coastal tundra (moist wet tundra) covered north of the Brooks Range between 11 and 10 ka,
438 where SP continued its expansion (Figure 8b). *Sphagnum*-black spruce forested peatland began
439 forming in southwestern coast and eastern interior regions, with a rapid increase of total peatland
440 area to about 13×10^5 km^2 (Figure 9). At 10-9 ka, boreal deciduous forest expanded to north of
441 the Brooks Range, making forest the dominant biome in Alaska (Figure 2c). Prevailing forest
442 ecosystems indicated a large expansion of peatland, with SBP covering the interior Alaska

(Figure 8c). During the mid-Holocene (9-5 ka), the terrestrial landscape generally resembled present-day ecosystems (Bigelow et al., 2003). Boreal evergreen needleleaf and mixed forest prevailed in southern and interior Alaska with tundra returned to north of the Brooks Range and western Alaska (Figures 2d and e). Although SP kept forming towards west, some areas dominated by SBP in interior Alaska ceased accumulating C (Figure 8d). At 5k-19th, almost all the peatlands have formed, with some interior regions exhibiting a C loss (Figure 8e). C accumulation increased again in the last century, averaging about 20 kg C m^{-2} kyr^{-1} (Figure 8f). We found that the distribution of SOC densities of both upland and peatland varied greatly depending on the vegetation distribution within each time slice, indicating that vegetation composition might be a major factor controlling regional C dynamics.

An average peat SOC "apparent" accumulation rate of 13 g C $m^{-2}yr^{-1}$ (2.3 Tg C yr^{-1} for the entire Alaska) was estimated from 15 ka to 2000 AD (Figure 10), lower than 18.6 g C $m^{-2}yr^{-1}$ as estimated from peat cores for northern peatlands (Yu et al., 2010), and slightly higher than the observed rate of 13.2 g C $m^{-2}yr^{-1}$ from four peatlands in Alaska (Jones and Yu, 2010). A simulated peak occurred during the HTM with the rate 29.1 g C $m^{-2}yr^{-1}$ (5.1 Tg C yr^{-1}), which was slightly higher than the observed 25 g C $m^{-2}yr^{-1}$ for northern peatlands and ~20 g C $m^{-2}yr^{-1}$ for Alaska (Yu et al., 2010). It was almost four times higher than the rate 6.9 g C $m^{-2}yr^{-1}$ (1.4 Tg C yr^{-1}) over the rest of the Holocene, which corresponded to the peat core-based observations of ~5 g C $m^{-2}yr^{-1}$. The mid- and late Holocene showed much slower C accumulation at a rate approximately five folds lower than during the HTM. This corresponded to the observation of a six-fold decrease in the rate of new peatland formation after 8.6 ka (Jones and Yu 2010). The C accumulation rates increased abruptly to 39.2 g C $m^{-2}yr^{-1}$during the last

465 century, within the field-measured average apparent rate range of 20-50 g C $m^{-2}yr^{-1}$ over the
466 last 2000 years (Yu et al., 2010).

467 The SOC stock of northern peatlands has been estimated in many studies, ranging from
468 210 to 621 Pg (Oechel 1989; Gorham 1991; Armentano and Menges, 1986; Turunen et al., 2002;
469 Yu et al., 2010; see Yu 2012 for a review). Assuming Alaskan peatlands were representative of
470 northern peatlands and using the area of Alaskan peatlands (0.45×10^6 km^2; Kivinen and
471 Pakarinen, 1981) divided by the total area of northern peatlnads (~4×10^6 km^2; Maltby and
472 Immirzi 1993), we estimated a SOC stock of 23.6-69.9 Pg C for Alaskan peatlands. Our model
473 estimated 27-48 Pg C (23.9 Pg C in SP and 13.5 Pg C in SBP) had been accumulated from 15 ka
474 to 2000 AD (Figure 11), due to uncertain parameters (Table 2~~4~~, see Wang et al. (2016) for model
475 parameters). The uncertainty can also be resulted from peat basal age distributions and the
476 estimation of total peatland area using modern inundation data as discussed above. By
477 incorporating the observed basal age distribution to determine the expansion of peatland through
478 time, we estimated that approximately 68% of Alaskan peatlands had formed by the end of the
479 HTM, similar to the estimation from observed basal peat ages that 75% peatlands have formed
480 by 8.6 ka (Jones and Yu 2010).

481 The northern circumpolar soils were estimated to cover approximately 18.78×10^6 km^2
482 (Tarnocai et al., 2009). The non-peatland soil C stock was estimated to be in the range of 150-
483 191 Pg C for boreal forests (Apps et al., 1993; Jobbagy and Jackson, 2000), and 60-144 Pg C for
484 tundra in the 0-100 cm depth (Apps et al., 1993; Gilmanov and Oechel, 1995; Oechel et al.,
485 1993). 1.24×10^6 km^2 non-peatland area was estimated from the total land area of Alaska
486 (1.69×10^6 km^2). Therefore, Alaska non-peatland soil contained 17-27 Pg C by using the ratio of

Alaskan over northern non-peatland. In comparison, we modeled 9-15 Pg C (within 1-meter depth), depending on the prior ranges of model parameters from Tang and Zhuang (2008).

The simulated modern SOC distribution (Figure 12c) was largely consistent with the study of Hugelius et al. (2014) (see Figure 3 in the paper). The model captured the SOC density on northern and southwestern coasts of Alaska with most grids >40 kg C m^{-2} on average. Those regions also showed high SOC density (>75 kg C m^{-2}), which was also exhibited in our result. East part and west coast had the lowest SOC densities, corresponding to the simulation result that most grids had SOC values between 20 and 40 kg C m^{-2}. We estimated an average peat depth of 1.9 ± 0.8 m considering the uncertainties within dry bulk densities. It was similar to the observed mean depth of 2.29 m for Alaskan peatlands (Gorham et al., 1991, 2012). Our estimates (Figure 12d) showed a relatively high correlation with the 64 observed peat samples, especially with higher depths (Figure 13) ($R^2 = 0.45$). The large intercept of the regression line (101 cm) suggested that the model might have not performed well in estimating the grids with low peat depths (<50 cm). The peat characteristics (e.g., bulk density) from location to location may differ largely, even if within the same small region. Thus, it is difficult to capture the observed variations of peat depths as we used the averaged bulk density of whole Alaska.

3.4 Effects of Climate on Ecosystem Carbon Accumulation

The simulated climate by ECBilt-CLIO model showed that among the six time periods, the coolest temperature appeared at 15-11 ka, followed by the mid- and late- Holocene (5 ka-1900 AD). Those two periods were also generally dry (Figure 3f). The former represented colder and drier climate before the onset of the Holocene and the HTM (Barber and Finney, 2000; Edwards

et al., 2001). The latter represented post-HTM neoglacial cooling, which has caused permafrost aggradation across northern high latitudes (Oksanen et al., 2001; Zoltai, 1995).

Despite ~~of~~ the relatively large inter-annual NPP variation ~~(Figure 5b) which was~~ resulted from the annual fluctuations of the climate forcing (Figure 5b), the~~The simulated~~ long-term NPP, vegetation C density and storage were highest during the HTM (Figure 5a and c). Annual C accumulation rates also reached the highest (Figures 5-11). The long-term variation of NPP has a similar pattern of the climate (see Figure 3 for climate variables), where higher NPP, along with higher vegetation C coincided with warmer temperatures and enhanced precipitation during the HTM, compared to other time periods. ECBilt-CLIO simulated a warmest summer and a prolonged growing season, leading to a stronger seasonality of temperature during the HTM (Kaufman et al., 2004, 2016), in line with the orbitally-induced maximum summer insolation (Berger and Loutre, 1991; Renssen et al., 2009). The coincidence between the highest vegetation C uptake and SOC accumulation rates and the warmest summer and the wetter-than-before conditions indicated a strong link between those climate variables and C dynamics in Alaska. Enhanced climate seasonality characterized by warmer summer, enhanced summer precipitation and possibly earlier snow melt during the HTM accelerated the photosynthesis and subsequently increased NPP (Tucker et al., 2001; Kimball et al., 2004; Linderholm, 2006). As shown in our sensitivity test, annual NPP was increased by 40 and 20 $g\ C\ m^{-2}\ yr^{-1}$ under the warmer and wetter scenarios, respectively (Figures 14a, b). Meanwhile, warmer condition could positively affect the SOC decomposition (Nobrega et al., 2007). However, it could be offset to a certain extent via the hydrological effect, as higher precipitation could raise the water-table position, allowing less space for aerobic heterotrophic respiration. Our sensitivity test results indicated that warmer and wetter conditions could lead to an increase of decomposition up to 35 and 15

531 g C m^{-2} yr^{-1}, respectively (Figures 14c, d). We did not find a decrease in total heterotrophic
532 respiration throughout Alaska from the higher precipitation. It was presumably due to a much
533 larger area of upland soils (1.3×10^6 km^2) than peatland soils (0.26×10^6 km^2), as higher
534 precipitation would cause higher aerobic respiration in the unsaturated zone of upland soils, and
535 consequently stimulated the SOC decomposition. The relatively low NPP and vegetation C
536 density, along with the lower total soil C stocks were consistent with the unfavorable cool and
537 dry climate conditions at 15-11 ka and during the mid- and late- Holocene. Statistical analysis
538 indicated that temperature had the most significant effect on peat SOC accumulation rate,
539 followed by the seasonality of NIRR (Wang et al., 2016). The seasonality of temperature, the
540 interaction of temperature and precipitation, and precipitation alone also showed significance.
541 The strong link between climate factors and C dynamics may explain the lower SOC
542 accumulation during the neoglacier cooling period (Marcott et al., 2013; Vitt et al., 2000; Peteet
543 et al., 1998; Yu et al. 2010). The rapid peat SOC accumulation during the 20th century under
544 warming and wetter climate may suggest a continuous C sink in this century, as concluded in
545 Spahni et al. (2013). However, the rising temperature in the future may have positive effects on
546 heterotrophic respiration and simultaneously increase evapotranspiration and lower water table.
547 This could increase aerobic decomposition and thus switch the Alaskan peatland from a C sink
548 into a C source. Moreover, the increasing anthropogenic activities including land use will
549 probably increase drought and subsequently enhance the risk of fire, releasing carbon to the
550 atmosphere. The fate of Alaskan SOC stock and the biogeochemical cycling of the terrestrial
551 ecosystems under future scenarios need further investigation.

552

553 **3.5 Effects of Vegetation Distribution on Ecosystem Carbon Accumulation**

554 Climate variables significantly affect C dynamics within each time slice. However,
555 different vegetation distributions during various periods led to clear step changes, suggesting
556 vegetation composition was likely to be another primary factor (Figures 6, 7, 8, and 11). As key
557 parameters controlling C dynamics in the model (e.g., maximum rate of photosynthesis, litter fall
558 C, maximum rate of monthly NPP) are ecosystem type specific, vegetation distribution changes
559 may drastically affect regional plant productivity and C storage. Our sensitivity test indicated
560 that by replacing all vegetation types with forests, there was a total increase of 36.9 Pg in upland
561 plus peatland soils. There was also an increase of 48.8 Pg C under warmer and wetter conditions,
562 suggesting that both climate and vegetation distribution may have played important roles in
563 carbon accumulation.

564 The vegetation changes reconstructed from fossil pollen data during different time
565 periods followed the general climate history during the last 15,000 years. For instance, the
566 migration of dark boreal forests over snow-covered tundra during the HTM was probably
567 induced by the warmer and wetter climate resulted from the insolation changes (He et al., 2014).
568 The cooler and drier climate after the mid-Holocene limited the growth of boreal broadleaf
569 conifers (Prentice et al., 1992), and therefore resulted in the replacement of broadleaf forest with
570 needleleaf forest and tundra ecosystems. Since the parameters of our model for individual
571 vegetation type were static, parameterizing the model using modern site-level observations might
572 have introduced uncertainty to parameters, which may result in regional simulation uncertainties.
573 Assuming each parameter as constant (e.g. the lowest water-table boundary, see Wang et al.
574 (2016) for details) over time may also weaken the model's response to different climate
575 scenarios. Furthermore, applying static vegetation maps at millennial scales and using modern
576 elevation and pH data may simplify the complicated changes of landscape and terrestrial

ecosystems, as vegetation can shift within hundreds of years (Ager and Brubake, 1985; see He et al. (2014) discussion section). Relatively coarse spatial resolution (0.5°×0.5°) in P-TEM simulations may also introduce uncertainties. In addition, because we used the modern inundation map to delineate the peatland and upland within each grid cell, we might have overestimated the total peatland area since not all inundated areas are peatlands. Linking field-estimated basal ages of peat cores to the vegetation types during each period involves large uncertainties due to the limitation of the peat classification and insufficient peat samples. Thus, the estimated spatially explicit basal age data shall also introduce a large uncertainty to our regional quantification of carbon accumulation.

4. Conclusions

We used a biogeochemistry model for both peatland and non-peatland ecosystems to quantify the C stock and its changes over time in Alaskan terrestrial ecosystems during the last 15,000 years. The simulated peat SOC accumulation rates were compared with peat-core data from four peatlands on the Kenai Peninsula in southern Alaska. The model well estimated the peat SOC accumulation rates trajectory throughout the Holocene. Our regional simulation showed that 36-63 Pg C had been accumulated in Alaskan land ecosystems since 15,000 years, including 27-48 Pg C in peatlands and 9-15 Pg C in non-peatlands (within 1 m depth). We also estimated that 2.5-3.7 Pg C was stored in contemporary Alaskan vegetation, with 0.3-0.6 Pg C in peatlands and 2.2-3.1 Pg C in non-peatlands. The estimated average rate of peat C accumulation was 2.3 Tg C yr^{-1} with a peak (5.1 Pg C yr^{-1}) in the Holocene Thermal Maximum (HTM), four folds higher than the rate of 1.4 Pg C yr^{-1} over the rest of the Holocene. The 20th century

represented another high SOC accumulation period after a much low accumulation period of the late Holocene. We estimated an average depth of 1.9 m of peat in current Alaskan peatlands, similar to the observed mean depth. ~~We found that~~ T~~t~~he changes of vegetation distribution were found to be the major control on~~the key factor to~~ the spatial variations of SOC accumulation in different time periods. The warming in the HTM characterized by the increased summer temperature and increased seasonality of solar radiation, as well as~~along with~~ the higher precipitation might have played an important role in the high C accumulation.

5. Acknowledgment. We acknowledge the funding support from a NSF project IIS-1027955 and a DOE project DE-SC0008092. We also acknowledge the SPRUCE project to allow us use its data. Data presented in this paper are publicly accessible: ECBilt-CLIO Paleosimulation (http://apdrc.soest.hawaii.edu/datadoc/sim2bl.php), CRU2.0 (http://www.cru.uea.ac.uk/data). Model parameter data and model evaluation process are in Wang et al. (2016). Other simulation data including model codes are available upon request from the corresponding author (qzhuang@purdue.edu).

6. References

Ager, T. A., & Brubaker, L.: Quaternary palynology and vegetational history of Alaska. Pollen Records of Late Quaternary North American Sediments, 353-384, 1985.

Apps, M. J., Kurz, W. A., Luxmoore, R. J., Nilsson, L. O., Sedjo, R. A., Schmidt, R., ... & Vinson, T. S.: Boreal forests and tundra. Water, Air, and Soil Pollution, 70(1-4), 39-53, 1993.

Armentano, T. V., & Menges, E. S.: Patterns of change in the carbon balance of organic soil-wetlands of the temperate zone. The Journal of Ecology, 755-774, 1986.

Assessment, A. C. I.: Forests, land management and agriculture.Arctic Climate Impact Assessment, 781-862, 2005.

Balshi, M. S., McGuire, A. D., Zhuang, Q., Melillo, J., Kicklighter, D. W., Kasischke, E., ... & Burnside, T. J.: The role of historical fire disturbance in the carbon dynamics of the pan-boreal region: A process-based analysis. Journal of Geophysical Research: Biogeosciences, 112(G2), 2007.

Barber, V. A., & Finney, B. P.: Late Quaternary paleoclimatic reconstructions for interior Alaska based on paleolake-level data and hydrologic models. Journal of Paleolimnology, 24(1), 29-41, 2000.

630 Belyea, L. R.: Nonlinear dynamics of peatlands and potential feedbacks on the climate
631 system. Carbon cycling in northern peatlands, 5-18, 2009.

632 Berger, A., & Loutre, M. F.: Insolation values for the climate of the last 10 million
633 years. Quaternary Science Reviews, 10(4), 297-317, 1991.

634 Bigelow, N. H., Brubaker, L. B., Edwards, M. E., Harrison, S. P., Prentice, I. C., Anderson, P.
635 M., ... & Kaplan, J. O.: Climate change and Arctic ecosystems: 1. Vegetation changes north of
636 55 N between the last glacial maximum, mid-Holocene, and present. Journal of Geophysical
637 Research: Atmospheres, 108(D19), 2003.

638 Bridgham, S. D., Megonigal, J. P., Keller, J. K., Bliss, N. B., & Trettin, C.: The carbon balance
639 of North American wetlands. Wetlands, 26(4), 889-916, 2006.

640 Carter, A. J., & Scholes, R. J.: SoilData v2. 0: generating a global database of soil
641 properties. Environmentek CSIR, Pretoria, South Africa, 2000.

642 Change, I. C.: Mitigation of Climate Change. Contribution of Working Group III to the Fifth
643 Assessment Report of the Intergovernmental Panel on Climate Change. Cambridge University
644 Press, Cambridge, UK and New York, NY, 2014.

645 Change, I. C.: The Physical Science Basis: Working Group I Contribution to the Fifth
646 Assessment Report of the Intergovernmental Panel on Climate Change. New York: Cambridge
647 University Press, 1, 535-1, 2013.

648 Chivers, M. R., Turetsky, M. R., Waddington, J. M., Harden, J. W., & McGuire, A. D.: Effects
649 of experimental water table and temperature manipulations on ecosystem CO2 fluxes in an
650 Alaskan rich fen.Ecosystems, 12(8), 1329-1342, 2009.

651 Churchill, A.: The response of plant community structure and productivity to changes in
652 hydrology in Alaskan boreal peatlands. Master Thesis, University of Alaska, Fairbanks, AK,
653 USA. 119 pp, 2011.

654 Conrad, R.: Contribution of hydrogen to methane production and control of hydrogen
655 concentrations in methanogenic soils and sediments.FEMS Microbiology Ecology, 28(3), 193-
656 202, 1999.

657 Davidson, E. A., & Janssens, I. A.: Temperature sensitivity of soil carbon decomposition and
658 feedbacks to climate change. Nature, 440(7081), 165-173, 2006.

659 Davidson, E. A., Trumbore, S. E., & Amundson, R.: Biogeochemistry: soil warming and organic
660 carbon content. Nature, 408(6814), 789-790, 2000.

661 Edwards, M. E., Mock, C. J., Finney, B. P., Barber, V. A., & Bartlein, P. J.: Potential analogues
662 for paleoclimatic variations in eastern interior Alaska during the past 14,000 yr: atmospheric-
663 circulation controls of regional temperature and moisture responses. Quaternary Science
664 Reviews, 20(1), 189-202, 2001.

665 Euskirchen, E. S., McGuire, A. D., & Chapin, F. S.: Energy feedbacks of northern high-latitude
666 ecosystems to the climate system due to reduced snow cover during 20th century
667 warming. Global Change Biology,13(11), 2425-2438, 2007.

668 Frolking, S., Roulet, N. T., Tuittila, E., Bubier, J. L., Quillet, A., Talbot, J., & Richard, P. J. H.:
669 A new model of Holocene peatland net primary production, decomposition, water balance, and
670 peat accumulation. Earth System Dynamics, 1(1), 1-21, 2010.

671 Frolking, S., Talbot, J., Jones, M. C., Treat, C. C., Kauffman, J. B., Tuittila, E. S., & Roulet, N.:
672 Peatlands in the Earth's 21st century climate system. Environmental Reviews, 19(NA), 371-396,
673 2011.

674 Gilmanov, T. G., & Oechel, W. C.: New estimates of organic matter reserves and net primary
675 productivity of the North American tundra ecosystems. Journal of Biogeography, 723-741, 1995.

676 Gorham, E. V. I. L. L. E.: Biotic impoverishment in northern peatlands. The earth in transition:
677 patterns and processes of biotic impoverishment. Cambridge University Press, Cambridge, UK,
678 65-98, 1990.

679 Gorham, E., Lehman, C., Dyke, A., Clymo, D., & Janssens, J.: Long-term carbon sequestration
680 in North American peatlands. Quaternary Science Reviews, 58, 77-82, 2012.

681 Gorham, E.: Northern peatlands: role in the carbon cycle and probable responses to climatic
682 warming. Ecological applications, 1(2), 182-195, 1991.

683 He, Y., Jones, M. C., Zhuang, Q., Bochicchio, C., Felzer, B. S., Mason, E., & Yu, Z.: Evaluating
684 CO 2 and CH 4 dynamics of Alaskan ecosystems during the Holocene Thermal
685 Maximum. Quaternary Science Reviews, 86, 63-77, 2014.

686 Hinzman, L. D., Viereck, L. A., Adams, P. C., Romanovsky, V. E., & Yoshikawa, K.: Climate
687 and permafrost dynamics of the Alaskan boreal forest. Alaska's Changing Boreal Forest, 39-61,
688 2006.

689 Hobbie, S. E.: Interactions between litter lignin and nitrogenitter lignin and soil nitrogen
690 availability during leaf litter decomposition in a Hawaiian montane forest. Ecosystems, 3(5),
691 484-494, 2000.

692 Hugelius, G., Strauss, J., Zubrzycki, S., Harden, J. W., Schuur, E., Ping, C. L., ... & O'Donnell, J.
693 A.: Estimated stocks of circumpolar permafrost carbon with quantified uncertainty ranges and
694 identified data gaps.Biogeosciences, 11(23), 6573-6593, 2014.

695 Jobbágy, E. G., & Jackson, R. B.: The vertical distribution of soil organic carbon and its relation
696 to climate and vegetation. Ecological applications, 10(2), 423-436, 2000.

697 Jones, M. C., & Yu, Z.: Rapid deglacial and early Holocene expansion of peatlands in
698 Alaska. Proceedings of the National Academy of Sciences,107(16), 7347-7352, 2010.

699 Jones, P. D., & Moberg, A.: Hemispheric and large-scale surface air temperature variations: An
700 extensive revision and an update to 2001. Journal of Climate, 16(2), 206-223, 2003.

701 Kane, E. S., Turetsky, M. R., Harden, J. W., McGuire, A. D., & Waddington, J. M.: Seasonal ice
702 and hydrologic controls on dissolved organic carbon and nitrogen concentrations in a boreal-rich
703 fen. Journal of Geophysical Research: Biogeosciences, 115(G4), 2010.

704 Kaufman, D. S., Ager, T. A., Anderson, N. J., Anderson, P. M., Andrews, J. T., Bartlein, P. J., ...
705 & Dyke, A. S.: Holocene thermal maximum in the western Arctic (0–180 W). Quaternary
706 Science Reviews, 23(5), 529-560, 2004.

707 Kaufman, D.S., Axford, Y.L., Henerson, A., McKay, N.P., Oswald, W.W., Saenger, C.,
708 Anderson, R.S., Bailey, H.L., Clegg, B., Gajewski, K., Hu, F.S., Jones, M.C., Massa, C.,
709 Routson, C.C., Werner, A., Wooller, M.J., Yu, Z.: Holocene climate changes in eastern Beringia
710 (NW North America) e a systemic review of multi-proxy evidence. Quaternary Science Reviews,
711 this volume. http://dx.doi.org/10.1016/ j.quascirev.2015.10.021, 2016.

712 Keller, J. K., & Bridgham, S. D.: Pathways of anaerobic carbon cycling across an ombrotrophic–
713 minerotrophic peatland gradient, 2007.

714 Keller, J. K., & Takagi, K. K.: Solid-phase organic matter reduction regulates anaerobic
715 decomposition in bog soil. Ecosphere, 4(5), 1-12, 2013.

716 Kimball, J. S., McDonald, K. C., Running, S. W., & Frolking, S. E.: Satellite radar remote
717 sensing of seasonal growing seasons for boreal and subalpine evergreen forests. Remote Sensing
718 of Environment, 90(2), 243-258, 2004.

719 Kivinen, E., and P. Pakarinen.: Geographical distribution of peat resources and major peatland
720 complex types in the world. Annales Academiae Scientarum Fennicae, Series A, Number 132,
721 1981.

722 Kleinen, T., Brovkin, V., & Schuldt, R. J.: A dynamic model of wetland extent and peat
723 accumulation: results for the Holocene.Biogeosciences, 9(1), 235-248, 2012.

724 Kuhry, P., & Vitt, D. H.: Fossil carbon/nitrogen ratios as a measure of peat
725 decomposition. Ecology, 77(1), 271-275, 1996.

726 Linderholm, H. W.: Growing season changes in the last century.Agricultural and Forest
727 Meteorology, 137(1), 1-14, 2006.

728 Loisel, J., Gallego-Sala, A. V., & Yu, Z.: Global-scale pattern of peatland Sphagnum growth
729 driven by photosynthetically active radiation and growing season length. Biogeosciences, 9(7),
730 2737-2746, 2012.

731 Loisel, J., Yu, Z., Beilman, D. W., Camill, P., Alm, J., Amesbury, M. J., ... & Belyea, L. R.: A
732 database and synthesis of northern peatland soil properties and Holocene carbon and nitrogen
733 accumulation. the Holocene, 0959683614538073, 2014.

734 Maltby, E., & Immirzi, P.: Carbon dynamics in peatlands and other wetland soils regional and
735 global perspectives. Chemosphere, 27(6), 999-1023, 1993.

736 Manabe, S., & Wetherald, R. T.: On the distribution of climate change resulting from an increase
737 in CO2 content of the atmosphere. Journal of the Atmospheric Sciences, 37(1), 99-118, 1980.

738 Manabe, S., & Wetherald, R. T.: Reduction in summer soil wetness induced by an increase in
739 atmospheric carbon dioxide. Science, 232(4750), 626-628, 1986.

740 Marcott, S. A., Shakun, J. D., Clark, P. U., & Mix, A. C.: A reconstruction of regional and global
741 temperature for the past 11,300 years.science, 339(6124), 1198-1201, 2013.

742 Matthews, E., & Fung, I.: Methane emission from natural wetlands: Global distribution, area,
743 and environmental characteristics of sources.Global biogeochemical cycles, 1(1), 61-86, 1987.

744 McGuire, A. D., & Hobbie, J. E.: Global climate change and the equilibrium responses of carbon
745 storage in arctic and subarctic regions. InModeling the Arctic system: A workshop report on the
746 state of modeling in the Arctic System Science program, pp. 53-54, 1997.

747 McGuire, A. D., Anderson, L. G., Christensen, T. R., Dallimore, S., Guo, L., Hayes, D. J., ... &
748 Roulet, N.: Sensitivity of the carbon cycle in the Arctic to climate change. Ecological
749 Monographs, 79(4), 523-555, 2009.

McGuire, A. D., Melillo, J. M., Kicklighter, D. W., & Joyce, L. A.: Equilibrium responses of soil carbon to climate change: empirical and process-based estimates. Journal of Biogeography, 785-796, 1995.

Melillo, J. M., Kicklighter, D. W., McGuire, A. D., Peterjohn, W. T., & Newkirk, K.: Global change and its effects on soil organic carbon stocks. In Dahlem Conference Proceedings, John Wiley and Sons, New York, John Wiley & Sons, Ltd., Chichster, pp. 175-189, 1995.

Mitchell, T. D., Carter, T. R., Jones, P. D., Hulme, M., & New, M.: A comprehensive set of high-resolution grids of monthly climate for Europe and the globe: the observed record (1901–2000) and 16 scenarios (2001–2100).Tyndall centre for climate change research working paper, 55(0), 25, 2004.

760 Moore, T. R., Bubier, J. L., Frolking, S. E., Lafleur, P. M., & Roulet, N. T.: Plant biomass and
761 production and CO2 exchange in an ombrotrophic bog. Journal of Ecology, 90(1), 25-36, 2002.

762 Nobrega, S., & Grogan, P.: Deeper snow enhances winter respiration from both plant-associated
763 and bulk soil carbon pools in birch hummock tundra. Ecosystems, 10(3), 419-431, 2007.

764 Oechel, W. C., Hastings, S. J., Vourlrtis, G., Jenkins, M., Riechers, G., & Grulke, N.: Recent
765 change of Arctic tundra ecosystems from a net carbon dioxide sink to a
766 source. Nature, 361(6412), 520-523, 1993.

767 Oechel, W. C.: Nutrient and water flux in a small arctic watershed: an overview. Holarctic
768 Ecology, 229-237, 1989.

769 Oksanen, P. O., Kuhry, P., & Alekseeva, R. N.: Holocene development of the Rogovaya river
770 peat plateau, European Russian Arctic.The Holocene, 11(1), 25-40, 2001.

771 Peteet, D., Andreev, A., Bardeen, W., & Mistretta, F.: Long-term Arctic peatland dynamics,
772 vegetation and climate history of the Pur-Taz region, western Siberia. Boreas, 27(2), 115-126,
773 1998.

774 Prentice, I. C., Cramer, W., Harrison, S. P., Leemans, R., Monserud, R. A., & Solomon, A. M.:
775 Special paper: a global biome model based on plant physiology and dominance, soil properties
776 and climate. Journal of biogeography, 117-134, 1992.

777 Raich, J. W., Rastetter, E. B., Melillo, J. M., Kicklighter, D. W., Steudler, P. A., Peterson, B.
778 J., ... & Vorosmarty, C. J.: Potential net primary productivity in South America: application of a
779 global model. Ecological Applications, 1(4), 399-429, 1991.

780 Renssen, H., Seppä, H., Heiri, O., Roche, D. M., Goosse, H., & Fichefet, T.: The spatial and
781 temporal complexity of the Holocene thermal maximum. Nature Geoscience, 2(6), 411-414,
782 2009.

783 Roulet, N. T., Lafleur, P. M., Richard, P. J., Moore, T. R., Humphreys, E. R., & Bubier, J. I. L.
784 L.: Contemporary carbon balance and late Holocene carbon accumulation in a northern
785 peatland. Global Change Biology, 13(2), 397-411, 2007.

786 Saarinen, T.: Biomass and production of two vascular plants in a boreal mesotrophic
787 fen. Canadian Journal of Botany, 74(6), 934-938, 1996.

788 Schuur, E. A., Bockheim, J., Canadell, J. G., Euskirchen, E., Field, C. B., Goryachkin, S. V., ...
789 & Mazhitova, G.: Vulnerability of permafrost carbon to climate change: implications for the
790 global carbon cycle.BioScience, 58(8), 701-714, 2008.

791 Sitch, S., Smith, B., Prentice, I. C., Arneth, A., Bondeau, A., Cramer, W., ... & Thonicke, K.:
792 Evaluation of ecosystem dynamics, plant geography and terrestrial carbon cycling in the LPJ
793 dynamic global vegetation model.Global Change Biology, 9(2), 161-185, 2003.

794 Spahni, R., Joos, F., Stocker, B. D., Steinacher, M., & Yu, Z. C.: Transient simulations of the
795 carbon and nitrogen dynamics in northern peatlands: from the Last Glacial Maximum to the 21st
796 century. Climate of the Past, 9(3), 1287-1308, 2013.

Stocker, B. D., Spahni, R., & Joos, F.: DYPTOP: a cost-efficient TOPMODEL implementation to simulate sub-grid spatio-temporal dynamics of global wetlands and peatlands. Geoscientific Model Development, 7(6), 3089-3110, 2014.

Stocker, B. D., Strassmann, K., & Joos, F.: Sensitivity of Holocene atmospheric CO 2 and the modern carbon budget to early human land use: analyses with a process-based model. Biogeosciences, 8(1), 69-88, 2011.

Tang, J., & Zhuang, Q.: A global sensitivity analysis and Bayesian inference framework for improving the parameter estimation and prediction of a process-based Terrestrial Ecosystem Model. Journal of Geophysical Research: Atmospheres, 114(D15), 2009.

Tang, J., & Zhuang, Q.: Equifinality in parameterization of process-based biogeochemistry models: A significant uncertainty source to the estimation of regional carbon dynamics. Journal of Geophysical Research: Biogeosciences, 113(G4), 2008.

Tang, J., Zhuang, Q., Shannon, R. D., & White, J. R.: Quantifying wetland methane emissions with process-based models of different complexities. Biogeosciences, 7(11), 3817-3837, 2010.

Tarnocai, C., Canadell, J. G., Schuur, E. A. G., Kuhry, P., Mazhitova, G., & Zimov, S.: Soil organic carbon pools in the northern circumpolar permafrost region. Global biogeochemical cycles, 23(2), 2009.

Timm, O., & Timmermann, A.: Simulation of the Last 21 000 Years Using Accelerated Transient Boundary Conditions*. Journal of Climate,20(17), 4377-4401, 2007.

Tucker, C. J., Slayback, D. A., Pinzon, J. E., Los, S. O., Myneni, R. B., & Taylor, M. G.: Higher northern latitude normalized difference vegetation index and growing season trends from 1982 to 1999. International journal of biometeorology, 45(4), 184-190, 2001.

Turetsky, M. R., Treat, C. C., Waldrop, M. P., Waddington, J. M., Harden, J. W., & McGuire, A. D.: Short-term response of methane fluxes and methanogen activity to water table and soil warming manipulations in an Alaskan peatland. Journal of Geophysical Research: Biogeosciences,113(G3), 2008.

Turunen, J., Tomppo, E., Tolonen, K., & Reinikainen, A.: Estimating carbon accumulation rates of undrained mires in Finland–application to boreal and subarctic regions. The Holocene, 12(1), 69-80, 2002.

Vitt, D. H., Halsey, L. A., Bauer, I. E., & Campbell, C.: Spatial and temporal trends in carbon storage of peatlands of continental western Canada through the Holocene. Canadian Journal of Earth Sciences, 37(5), 683-693, 2000.

Wang, S., Zhuang, Q., Yu, Z., Bridgham, S., & Keller, J. K.: Quantifying peat carbon accumulation in Alaska using a process-based biogeochemistry model, Journal of Geophysical Research: Biogeosciences., 121, doi: 10.1002/2016JG003452, 2016.

XU-RI and PRENTICE, I. C.: Terrestrial nitrogen cycle simulation with a dynamic global vegetation model. Global Change Biology, 14: 1745–1764. doi:10.1111/j.1365-2486.2008.01625.x, 2008.

Yu, Z. C.: Northern peatland carbon stocks and dynamics: a review. Biogeosciences, 9(10), 4071-4085, 2012.

Yu, Z., Beilman, D. W., & Jones, M. C.: Sensitivity of northern peatland carbon dynamics to Holocene climate change. Carbon cycling in northern peatlands, 55-69, 2009.

Yu, Z., Loisel, J., Brosseau, D. P., Beilman, D. W., & Hunt, S. J.: Global peatland dynamics since the Last Glacial Maximum. Geophysical Research Letters, 37(13), 2010.

Zhuang, Q., McGuire, A. D., Melillo, J. M., Clein, J. S., Dargaville, R. J., Kicklighter, D. W., ... & Hobbie, J. E.: Carbon cycling in extratropical terrestrial ecosystems of the Northern Hemisphere during the 20th century: a modeling analysis of the influences of soil thermal dynamics. Tellus B, 55(3), 751-776, 2003.

Zhuang, Q., McGuire, A. D., O'neill, K. P., Harden, J. W., Romanovsky, V. E., & Yarie, J.: Modeling soil thermal and carbon dynamics of a fire chronosequence in interior Alaska. Journal of Geophysical Research: Atmospheres, 107(D1), 2002.

Zhuang, Q., Melillo, J. M., Kicklighter, D. W., Prinn, R. G., McGuire, A. D., Steudler, P. A., ... & Hu, S.: Methane fluxes between terrestrial ecosystems and the atmosphere at northern high latitudes during the past century: A retrospective analysis with a process-based biogeochemistry model. Global Biogeochemical Cycles, 18(3), 2004.

Zhuang, Q., Melillo, J. M., McGuire, A. D., Kicklighter, D. W., Prinn, R. G., Steudler, P. A., ... & Hu, S.: Net emissions of CH4 and CO2 in Alaska: Implications for the region's greenhouse gas budget. Ecological Applications, 17(1), 203-212, 2007.

Zhuang, Q., Romanovsky, V. E., & McGuire, A. D.: Incorporation of a permafrost model into a large-scale ecosystem model: Evaluation of temporal and spatial scaling issues in simulating soil thermal dynamics.Journal of Geophysical Research: Atmospheres, 106(D24), 33649-33670, 2001.

Zhuang, Q., Zhu, X., He, Y., Prigent, C., Melillo, J. M., McGuire, A. D., ... & Kicklighter, D. W.: Influence of changes in wetland inundation extent on net fluxes of carbon dioxide and methane in northern high latitudes from 1993 to 2004. Environmental Research Letters, 10(9), 095009, 2015.

Zimov, S. A., Schuur, E. A., & Chapin III, F. S.: Permafrost and the global carbon budget. Science(Washington), 312(5780), 1612-1613, 2006.

Zoltai, S. C.: Permafrost distribution in peatlands of west-central Canada during the Holocene warm period 6000 years BP. Géographie physique et Quaternaire, 49(1), 45-54, 1995.

Table 1. Description of sites and variables used for parameterizing the core carbon and nitrogen module (CNDM).

Site[a]	Vegetation	Observed variables for CNDM parameterization	References
APEXCON	Moderate rich open fen with sedges (*Carex* sp.), spiked rushes (*Eleocharis* sp.), *Sphagnum* spp., and brown mosses (e.g., *Drepanocladus aduncus*)	Mean annual aboveground NPP in 2009; Mean annual belowground NPP in 2009; Aboveground biomass in 2009	Chivers et al. (2009) Turetsky et al. (2008) Kane et al. (2010) Churchill et al. (2011)
APEXPER	Peat plateau bog with black spruce (*Picea mariana*), *Sphagnum* spp., and feather mosses		

[a]The Alaskan Peatland Experiment (APEX) site is adjacent to the Bonanza Creek Experimental Forest (BCEF) site, approximately 35 km southwest of Fairbanks, AK. The area is classified as continental boreal climate with a mean annual temperature of -2.9℃ and annual precipitation of 269 mm, of which 30% is snow (Hinzman et al., 2006).

Table 2. Carbon pools and fluxes used for calibration of CMDM

Annual Carbon Fluxes or Pools[a]	*Sphagnum* Open Fen		*Sphagnum*-Black Spruce Bog		References
	Observation	Simulation	Observation	Simulation	
NPP	445±260	410	433±107	390	Turetsky et al. (2008), Churchill (2011)
Aboveground Vegetation Carbon	149-287		423		Saarinen et al. (1996)
Belowground Vegetation Carbon	347-669		987		Moore et al. (2002)
Total Vegetation Carbon Density	496-856	800	1410	1300	Zhuang et al. (2002)
Litter Fall Carbon Flux	300	333	300	290	Tarnocai et al. (2009)
Methane Emission Flux	19.5	19.2	9.7	12.8	Kuhry and Vitt (1996)

[a] Units for annual net primary production (NPP) and litter fall carbon are $g\ C\ m^{-2}\ yr^{-1}$. Units for vegetation carbon density are $g\ C\ m^{-2}$. Units for Methane emissions are $g\ C-CH_4\ m^{-2}\ yr^{-1}$. The simulated total annual methane fluxes were compared with the observations at APEXCON in 2005 and SPRUCE in 2012. A ratio of 0.47 was used to convert vegetation biomass to carbon (Raich 1991).

898 Table 3. Assignment of biomized fossil pollen data to the vegetation types in TEM (He et al.,
899 2014).

TEM upland vegetation	TEM peatland vegetation	BIOMISE code
Alpine tundra		CUSH DRYT PROS
Moist tundra	*Sphagnum* spp. open fen	DWAR SHRU
Boreal evergreen needleleaf and mixed forest	*Sphagnum*-black spruce bog	TAIG COCO CLMX COMX
Boreal deciduous broadleaf forest		CLDE

900

901

902 Table 4. Relations between peatland basal age and vegetation distribution

Peatland basal age	Vegetation types	Location in Alaska
15-11 ka	alpine tundra	south, northwestern, and southeastern coast
11-10 ka	moist tundra	south, north, and southeastern coast
	boreal evergreen needleleaf forest	
	boreal deciduous broadleaf forest	east central part
10-9 ka	moist tundra	south and north coast
	boreal evergreen needleleaf forest	central part
	boreal deciduous broadleaf forest	
9-5 ka	moist tundra	central part
	boreal evergreen needleleaf forest	
5 ka-1900 AD	moist tundra	west coast
	boreal evergreen needleleaf forest	

903

904

905

906

907

908

909

910

911

912

913

Table 5. Sites used for comparison of carbon accumulation rates between simulation and observation [*Jones and Yu*, 2010]

Site name	Location	Peatland type	Latitude	Longitude	Dating method	No. of dates	Basal age (cal yr BP)	Time-weighted Holocene accumulation rates (g C m^{-2} yr^{-1})
Kenai Gasfield	Alaska, USA	fen	60º27'N	151º14'W	AMS	12	11,408	13.1
No Name Creek	Alaska, USA	fen	60º38'N	151º04'W	AMS	11	11,526	12.3
Horsetrail fen	Alaska, USA	rich fen	60º25'N	150º54'W	AMS	10	13,614	10. 7
Swanson fen	Alaska, USA	poor fen	60º47'N	150º49'W	AMS	9	14,225	5.7

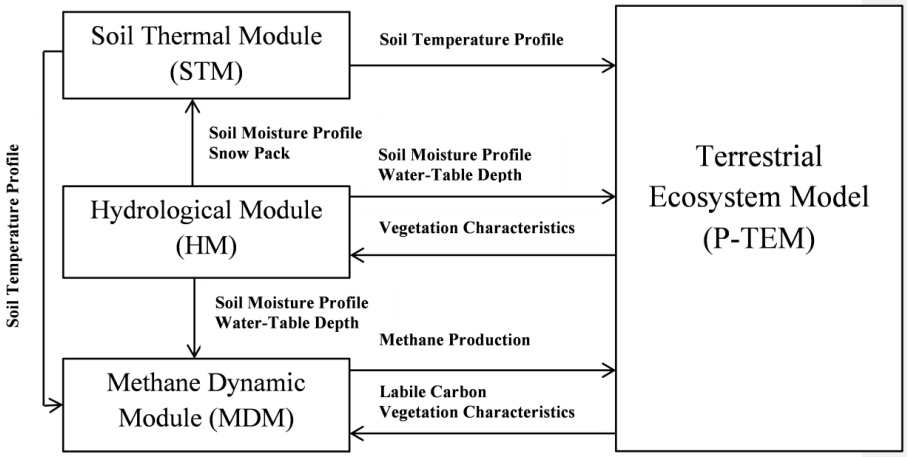

Figure 1. P-TEM (Peatland-Terrestrial Ecosystem Model) framework includes a soil thermal module (STM), a hydrologic module (HM), a carbon/ nitrogen dynamic model (CNDM), and a methane dynamics module (MDM) (Wang et al., 2016).

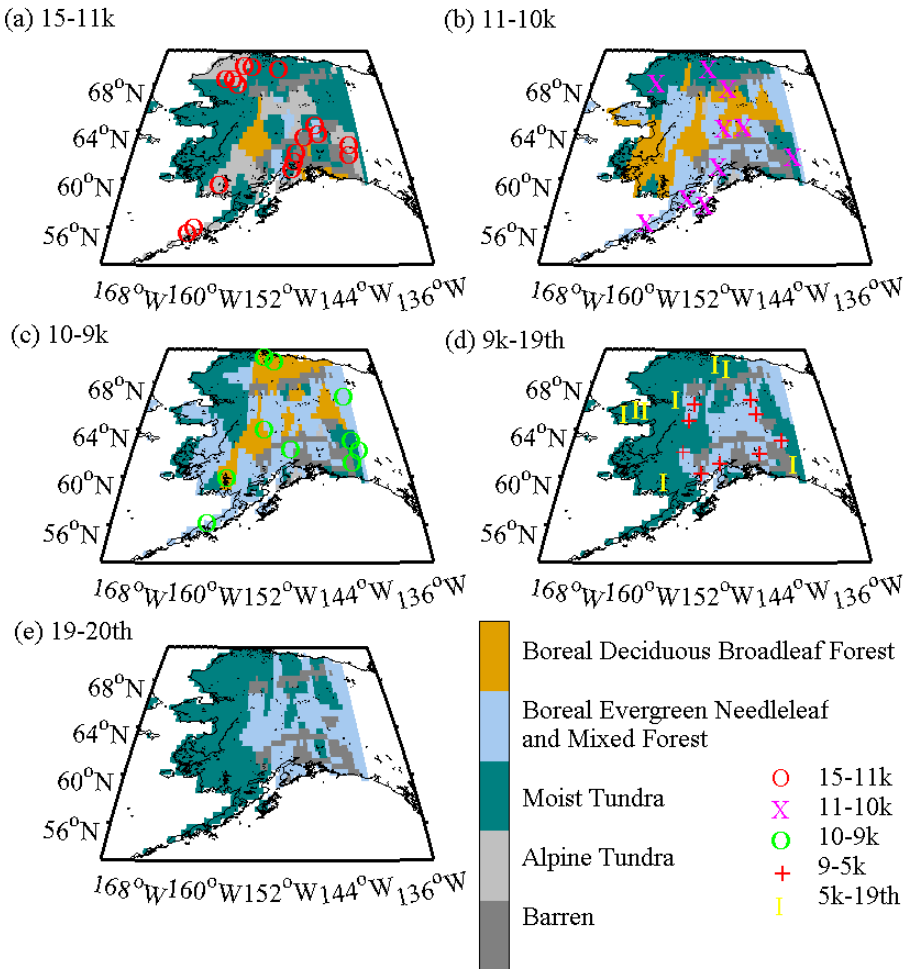

Figure 2. Alaskan vegetation distribution maps reconstructed from fossil pollen data during (a) 15-11 ka, (b) 11-10 ka, (c) 10-9 ka, (d) 9 ka -1900 AD, and (e) 1900-2000 AD (He et al., 2014). Symbols represent the basal age of peat samples (n = 102) in Gorham et al. (2012). Each symbol indicates 1-3 peat samples in the map. Peat samples with basal age 9-5k and 5k-19th are shown in map (d) as there is no change of vegetation distribution during 9k-19th. Barren refers to mountain range and large water body areas that can not be interpolated.

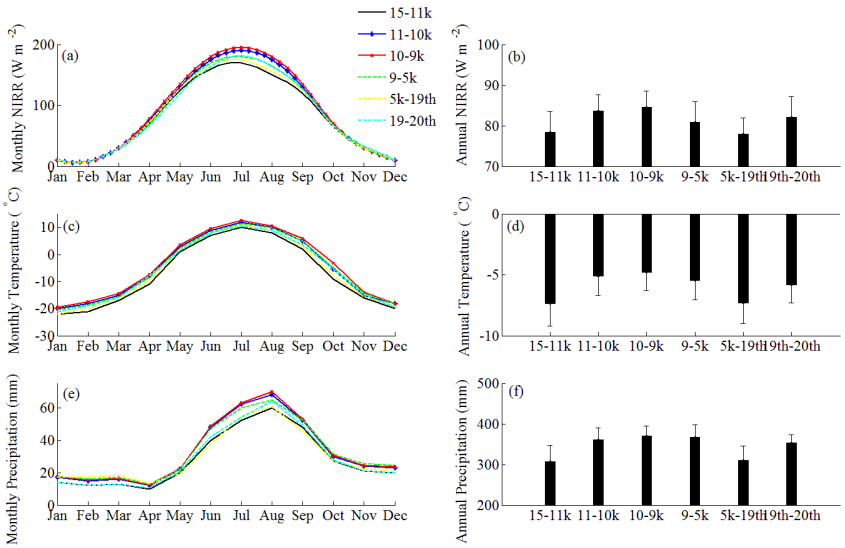

Figure 3. Simulated Paleo-climate and other input data from 15 ka to 2000 AD: (a) mean monthly and (b) mean annual net incoming solar radiation (NIRR, W m^{-2}), (c) mean monthly and (d) mean annual air temperature (℃), (e) mean monthly, and (f) mean annual precipitation (mm) (Timm and Timmermann, 2007; He et al., 2014).

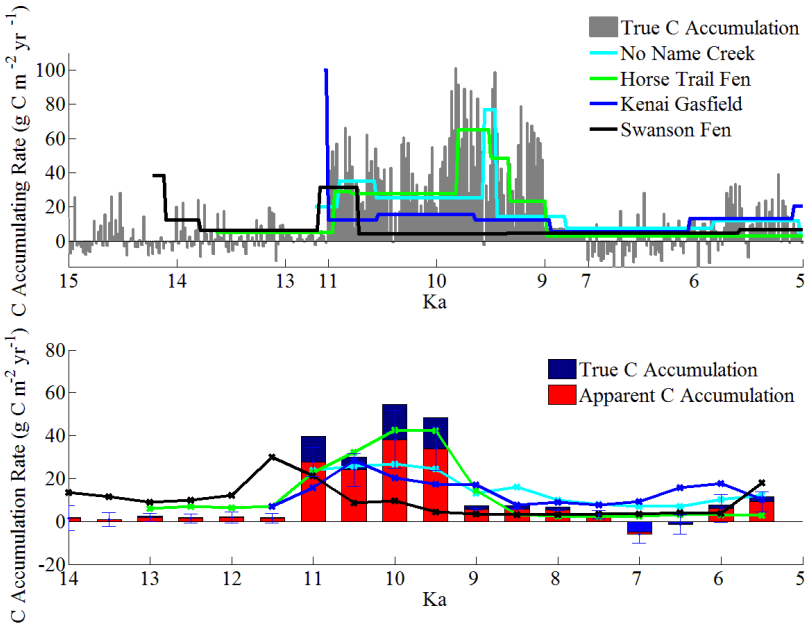

965

Formatted: Font: (Default) Times New Roman, (Asian) Times New Roman, 0 pt, Font color: Black, Character scale: 0%, Border: : (No border), Pattern: Clear (Black)

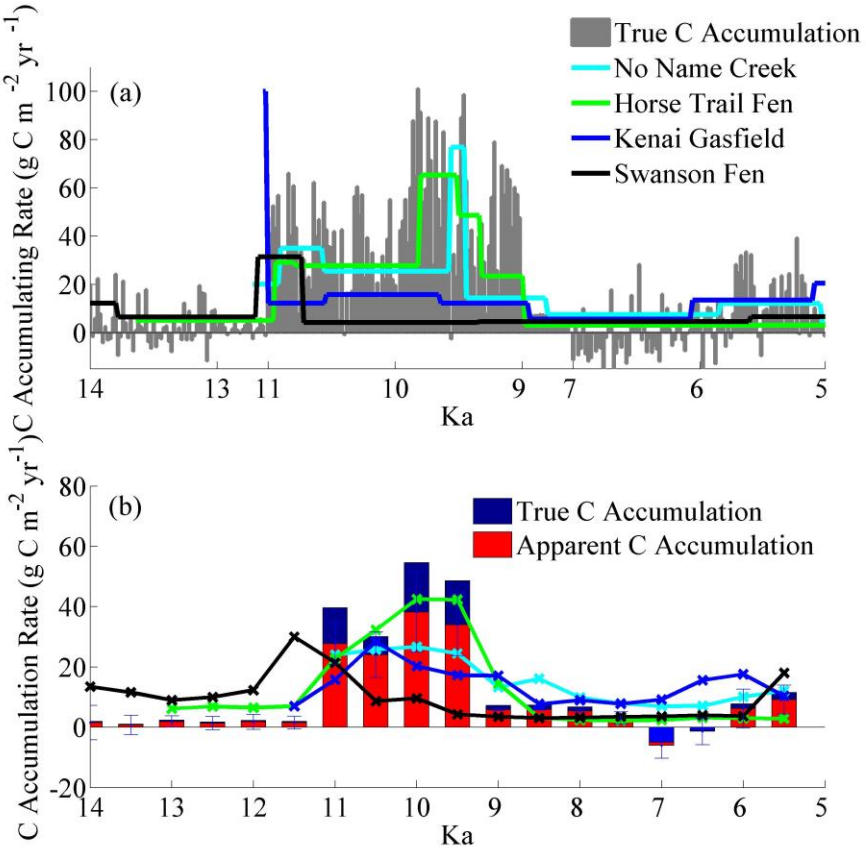

Figure 4. Simulated and observed carbon accumulation rates from 15 ka to 5 ka in 20-yr bins (a) and 500-yr bins with standard deviation (b) for No Name Creek, Horse Trail Fen, Kenai Gasfield, and Swanson Fen. Peat-core data were from Jones and Yu (2010).

976

977

978

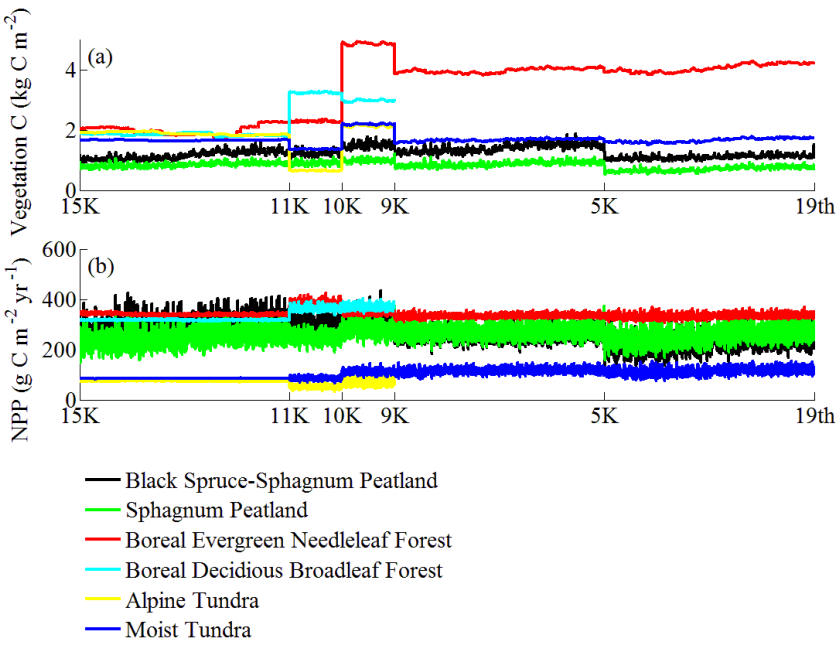

979

Formatted: Font: (Default) Times New Roman, 小四

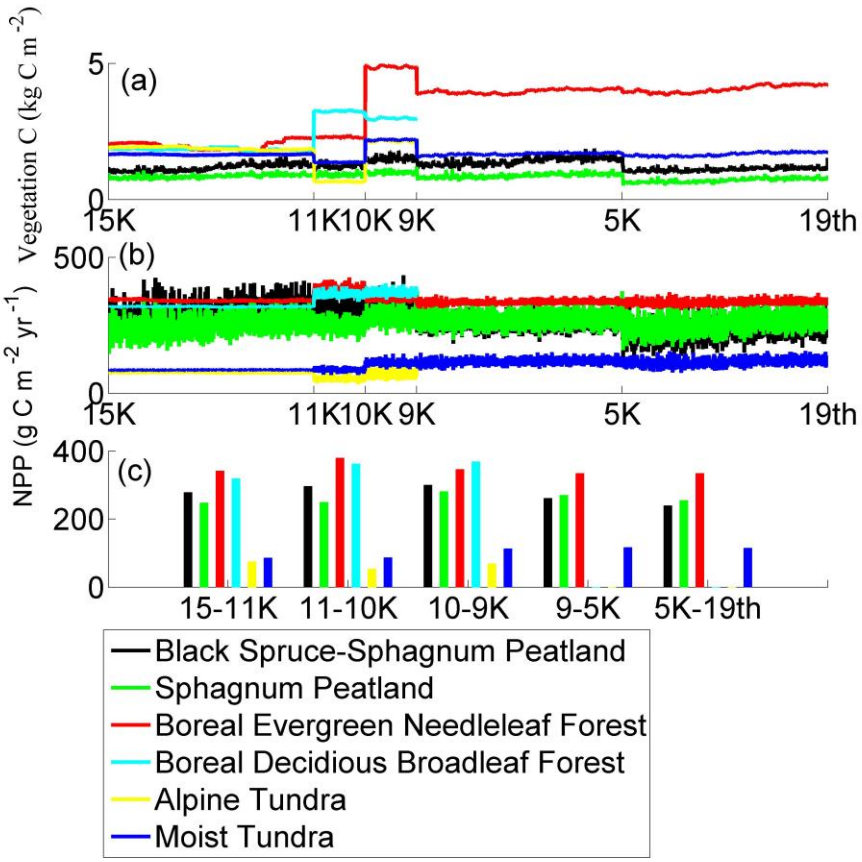

Figure 5. Simulated (a) mean vegetation carbon density (kg C m^{-2}) of different vegetation types, ~~and~~ (b) annual NPP (g C $m^{-2}yr^{-1}$)~~.~~, and (c) long-term NPP (g C $m^{-2}yr^{-1}$).

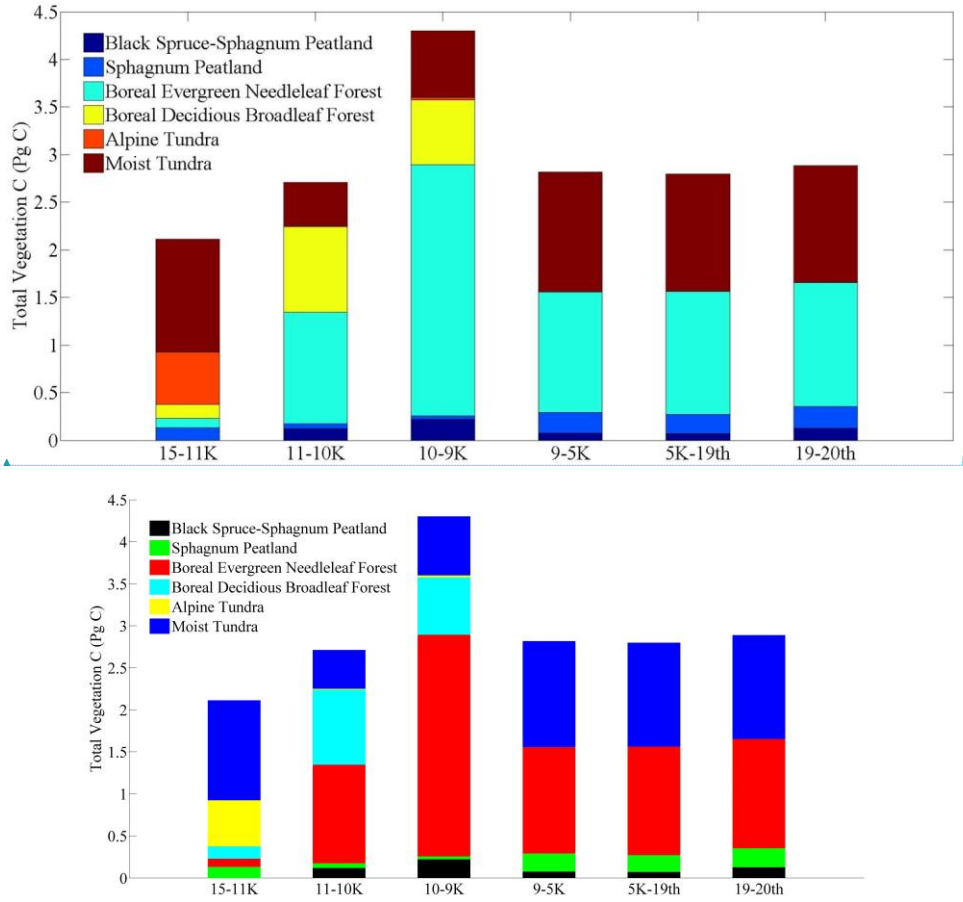

Figure 6. Total C (Pg C) stored in Alaskan vegetation for different time periods.

Formatted: Font: (Default) Times New Roman, 小四

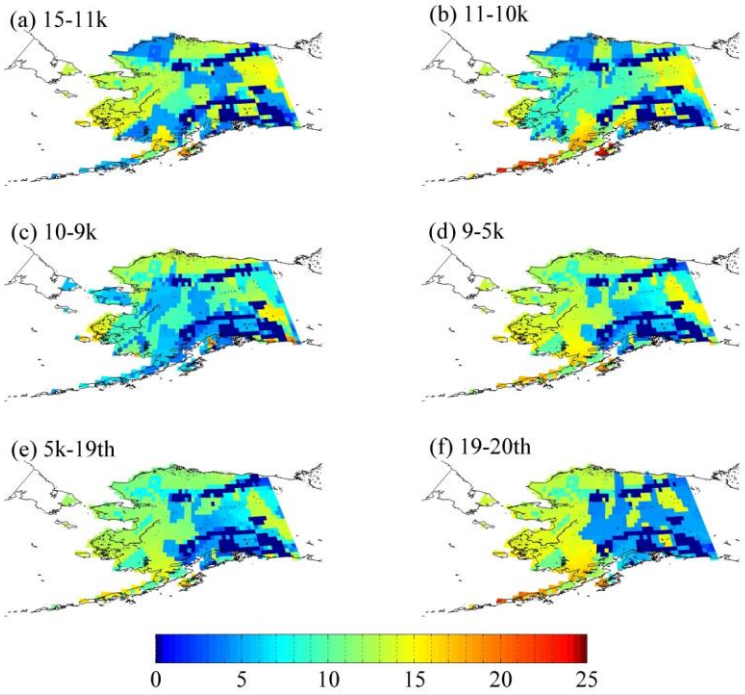

990

Formatted: Font: (Default) Times New Roman, 小四

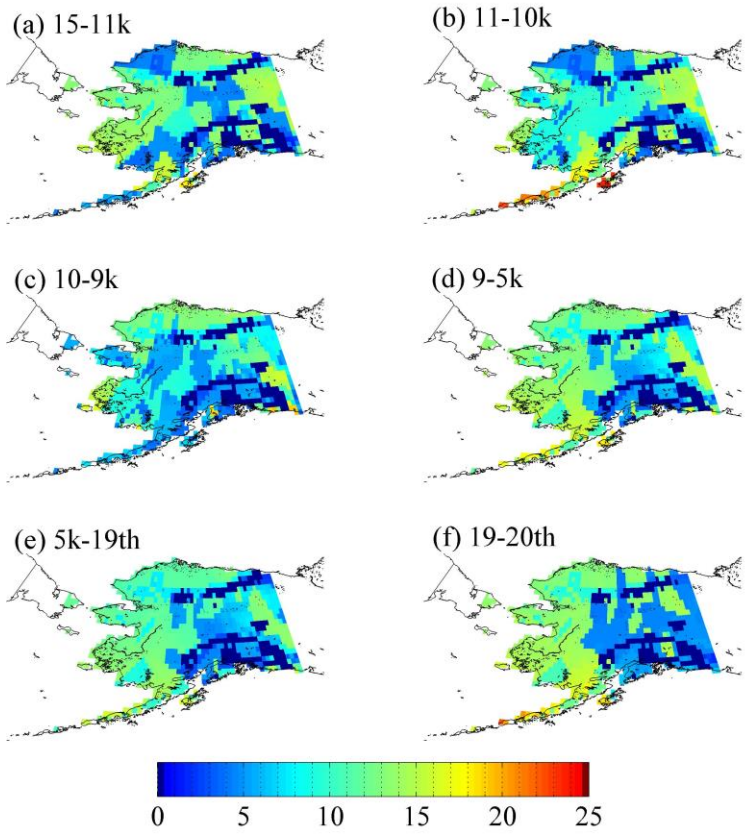

Figure 7. Average non-peatland (mineral) SOC density (kg C m^{-2}) during (a) 15-11 ka, (b) 11-10 ka, (c) 10-9 ka, (d) 9-5 ka, (e) 5 ka -1900 AD, and (f) 1900-2000 AD. The period of 9k-19th in Figure 2d is separated into 9-5k and 5k-19th.

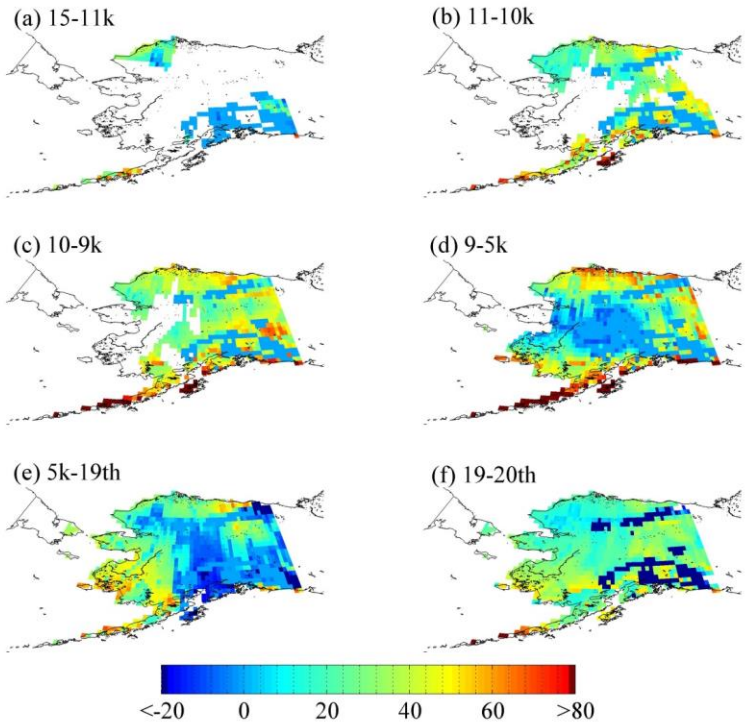

Figure 8. Peatland area expansion and peat soil C accumulation per 1000 years (kg C m^{-2} kyr^{-1}) during (a) 15-11 ka, (b) 11-10 ka, (c) 10-9 ka, (d) 9-5 ka, (e) 5 ka -1900 AD, and (f) 1900-2000 AD. The amount of C represents the C accumulation as the difference between the peat C amount in the final year and the first year in each time slice. The period of 9k-19th in Figure 2d is separated into 9-5k and 5k-19th.

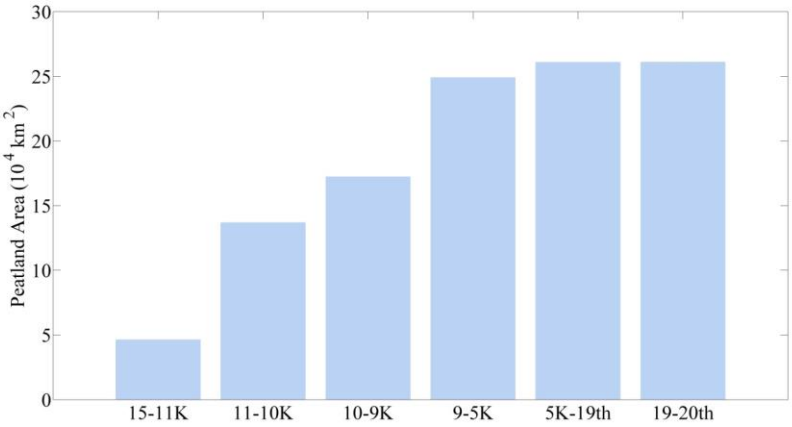

Figure 9. Peatland expansion area (10^4 km^2) in different time slices.~~, the area of barren in the map is set to 0 km^2.~~

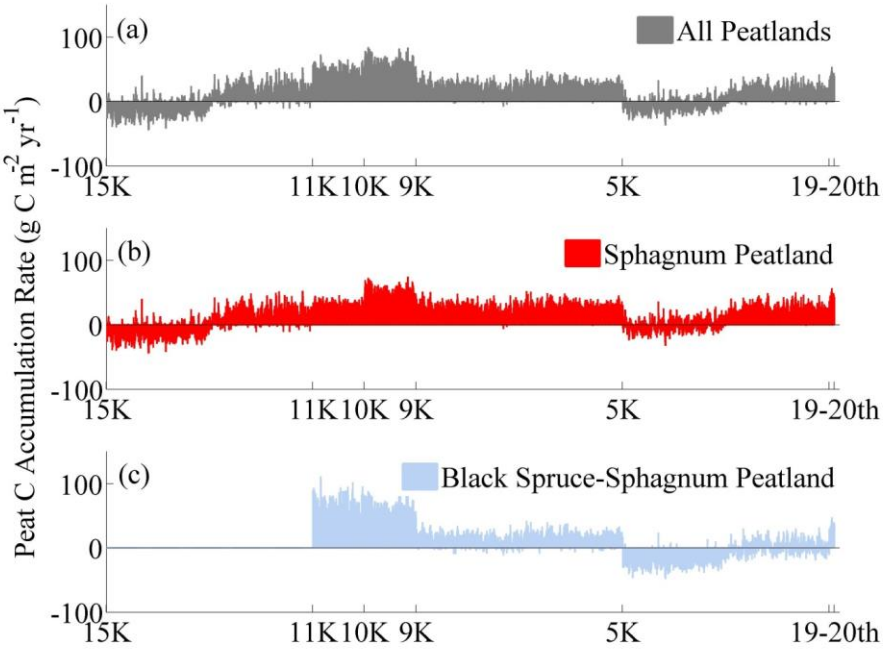

Figure 10. Bars of p~~P~~eatland mean C accumulation rates from 15 ka to 2000 AD for (a) weighted average of all peatlands, (b) *Sphagnum* open peatlands, and (c) *Sphagnum*-black spruce peatlands.

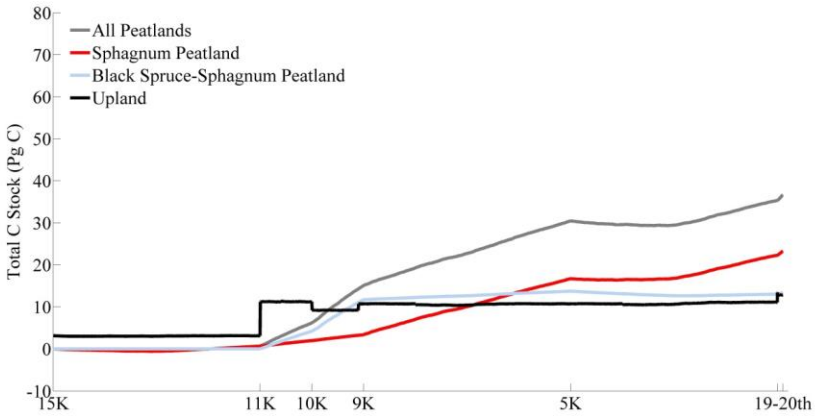

Figure 11. Total C stock accumulated from 15 ka to 2000 AD for all peatlands, *Sphagnum* open peatlands, *Sphagnum*-black spruce peatlands, and upland soils.

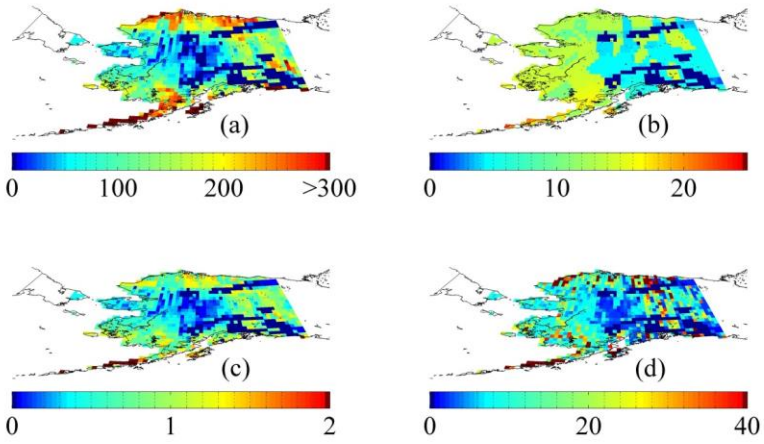

Figure 12. Spatial distribution of (a) total peat SOC density (kg C m^{-2}), (b) total mineral SOC density (kg C m^{-2}), (c) total peat depth (m), and (d) area-weighted total (peatlands plus non-peatlands) SOC density (kg C m^{-2}) in Alaska from 15 ka to 2000 AD.

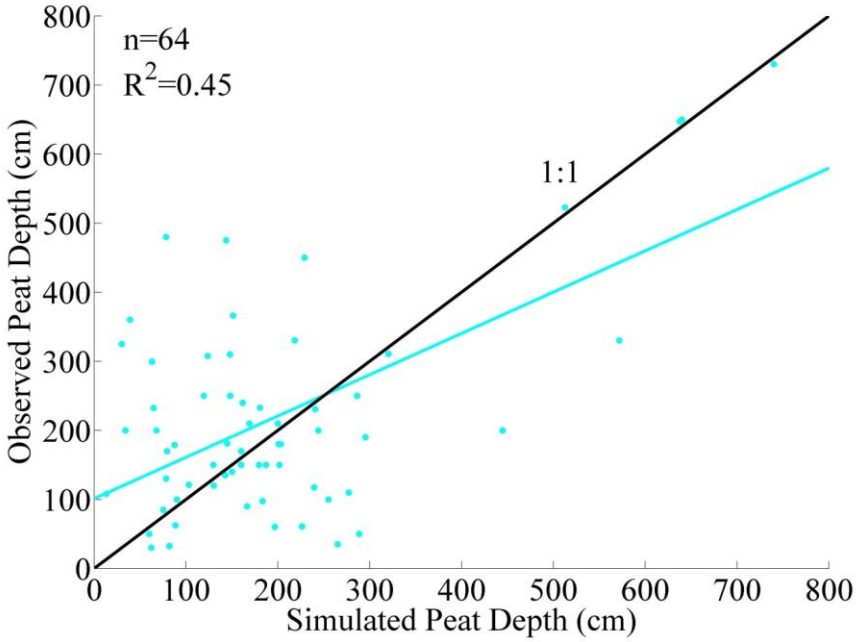

Figure 13. Field-based estimates and model simulations for peat depths in Alaska: The observed and simulated data are extracted from the same grids on the map. Linear regression line (cyan) is compared with the 1:1 line. The linear regression is significant ($P<0.001$, $n = 64$) with $R^2 = 0.45$, slope = 0.65, and intercept = 101.05 cm. The observations of >1000 cm are treated as outliers.

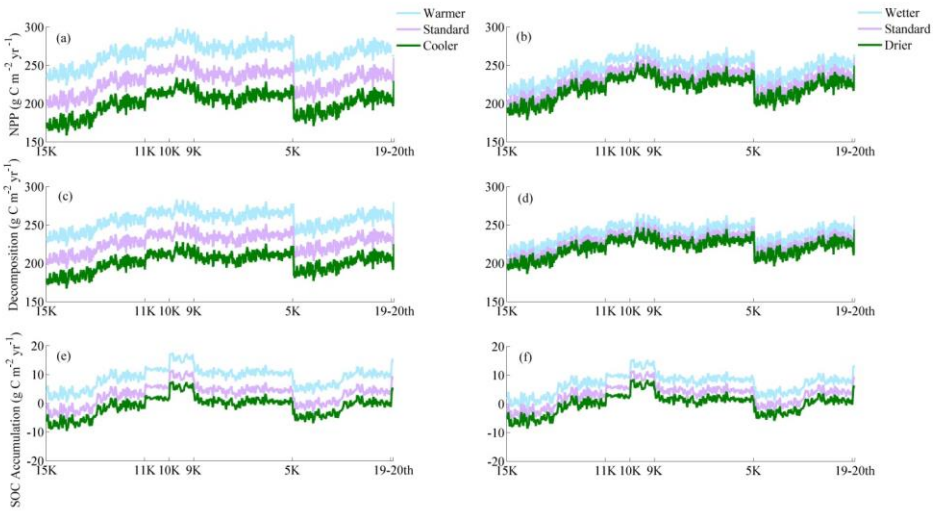

Figure 14. Temperature and precipitation effects on (a)(b) annual NPP, (c)(d) annual SOC decomposition rate (aerobic plus anaerobic), and (e)(f) annual SOC accumulation rate of Alaska. A 10-year moving average was applied.